NUMERICAL SIMULATION OF NO_x EMISSION CHARACTERISTICS DURING COMBUSTION IN 350 MW SUPERCRITICAL COGENERATION TANGENTIALLY BOILER

by

Wei-Shu WANG[a*], Zhi-Hao HUANG[a], Miao TIAN[a], Ji-Hong WANG[b], Shan-Shan SHANGGUAN[a], and Ming-Yu YAO[c]

[a]Thermal Engineering Research Center,
North China University of Water Resources and Electric Power, Zhengzhou, China
[b]Linzhou Thermal Power Co., Ltd of Datang. Linzhou, China
[c]Xi'an Thermal Power Research Institute Co., Ltd, Xi'an, China

Original scientific paper
https://doi.org/10.2298/TSCI191010006W

In light of a 350 MW supercritical cogeneration tangential boiler, the combustion and the NO_x release mechanism in the furnace were numerically simulated. The combustion characteristics were analyzed, and the influencing factors, such as the pulverized coal concentration, the velocity of separated over-fire air and the boiler load, on NO_x release in the furnace were also systematically studied. The results show that the central air-flow in the furnace rises spirally, and an inverted V-type temperature distribution is formed. The generation of NO_x can be effectively restrained by increasing the concentration of pulverized coal properly. Compared with the conventional concentration, the concentration of NO_x at the furnace exit can be reduced by 29.63% by taking high pulverized coal concentration. The concentration of NO_x at the furnace exit can be drastically reduced by increasing the velocity of separated over-fire air. When decreasing boiler load, the concentration of NO_x at furnace exit declines at first and then increases.

Key words: *supercritical cogeneration tangential boiler, pulverized coal concentration, separated over-fire air, boiler load, NO_x emission, numerical simulation*

Introduction

Combined heat and power (CHP) is one of the key energy-saving projects, in which energy can be used effectively. Supercritical cogeneration can significantly improve energy conversion efficiency, and steady progress has been made in promoting supercritical cogeneration [1-4]. In the new era, the nitrogen/sulfur emission control of cogeneration is more stringent, and the NO_x emissions from the supercritical cogeneration boiler unit are extremely important [5-8].

Tangentially-firing is widely used in supercritical boilers because of the supply and cost control of electric coal. However, most of the boilers in China are heavily deflected from the design coal, and some problems exist in tangentially-firing boiler burning the low-reactive

*Corresponding author, email: wangweishu@ncwu.edu.cn

coal, such as the flame deflection, high temperature difference of flue gas, poor combustion performance of low load and high NO_x emissions at the furnace outlet, which seriously threatens the safe and clean operation of boilers [1-4]. Numerical simulation and test methods are usually used for the study of NO_x control in the tangentially-firing boiler [9-11]. In the early stage of the coal combustion and NO_x product (*e.g.* HCN and NH_3), the precipitation characteristics of basic research showed that the NO_x conversion mechanism was complex [12, 13]. There are many parameters influencing the release of NO_x, such as coal powder concentration, temperature, and fuel characteristics. Experimental study on specific objects and conditions can optimize combustion to achieve coal combustion and NO_x suppression [10, 11]. Wang *et al.* [14] experimentally investigated the influence of coal powder ratio, structure and operation parameters on nitrogen precipitation and the release rule of NO_x. The experimental study of Wang *et al*. [15] and Jarguin-Lopez *et al*. [16] showed that the boiler structure, the type of burner and the method of coal burning have a significant influence on NO_x emission. Xiao *et al*. [17] studied the effects of oxygen quantity and air distribution on NO_x emission in the 1025 t/h boiler and found that the adjustment of coal combustion could significantly reduce the concentration of NO_x. Zhou *et al*. [18] studied air classification and dense-lean combustion and inhibited NO_x generation through the optimization of air distribution. Li *et al*. [19] and Zheng *et al*. [20] studied the effects of secondary air on the combustion and the release of NO_x of a subcritical 300 MW boiler. However, the results showed that the effects of secondary air were not obvious. With the development of computer technology, numerical simulation has been used to solve the study of the combustion of boilers and the release and control of nitrogen/sulfur pollutants [21, 22]. Choi and Chang [23] numerically simulated the flow, combustion and NO_x release of 500 MW tangentially fired furnace. Chen *et al*. [24] has simulated the synergistic effect of boiler structure effect, burner type and air distribution. Wang *et al*. [25] and Liu *et al*. [26] applied the numerical simulation technology to the study of the combustion and NO_x release of the supercritical W-shaped boiler with lean coal, which provides technical support for the supercritical development of W flame boiler.

In order to meet the efficient and clean operation of the supercritical cogeneration tangential boiler software FLUENT 6.3 was used to study the combustion and NO_x generation rules of a 350 MW supercritical cogeneration tangentially boiler. The influence of coal concentration, air distribution and variable load on NO_x generation was analyzed to reduce the release of NO_x. The results could provide guidance for the operation of the units.

Physical model and numerical simulation

Physical model

In this paper, a 350 MW supercritical parameter CHP unit in Linzhou Thermal Power Co., Ltd of Datang was studied, and the operating conditions and simulation results were compared. The width of the furnace is 13608 mm, and the depth is 12798 mm. Tangential combustion and the oscillating burner is arranged on every angle of the furnace. As shown in fig. 1, The primary air and the secondary air, both five layers, are alternately arranged, and a layer of closed coupled over fire air and three layers of separated over fire air are arranged near-

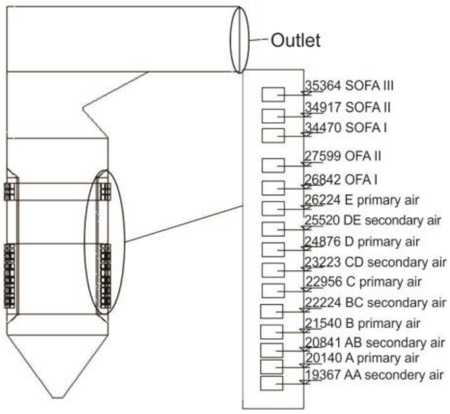

Figure 1. Structure diagram

by. The coal air-flow is heated by the radiation convection and heat transfer in the furnace after entering the furnace from a wind nozzle and reaches the ignition and combustion condition. The designed coal is lean coal in Shanxi Province, and the characteristics of coal are listed in tab. 1.

Table 1. The designed characteristics of fuel coal

Industry analysis			Elemental analysis					Calorific value
V_{daf} [%]	M_{ad} [%]	A_{ar} [%]	C_{ar} [%]	H_{ar} [%]	N_{ar} [%]	O_{ar} [%]	S_{ar} [%]	$Q_{net,ar}$ [MJkg^{-1}]
16.60	0.80	29.45	54.30	2.63	0.79	2.75	2.08	20.45

In this paper, the release rules of NO_x with different coal concentrations, different combustion wind velocity and different loads were studied, and the simulated conditions are listed in tab. 2.

Table 2. Simulated condition summary table

The wind type		The air velocity [ms^{-1}]			
		Primary air	Second air	Over fire air	Separated over fire air
Original condition	/	22	42	51	43
Change the air velocity	Condition 1	22	50	51	33
	Condition 2	22	46	51	38
	Condition 3	22	38	51	48
Different load	80%	22	33.6	40.8	34.4
	50%	22	21	25.5	21.5

General

A 1:1 model of the furnace was established and the calculation boundary is from the cold ash hopper to the furnace outlet area. The grid was divided into three parts using software GAMBIT 2.4.6. Because of the complexity of the calculation area of the flow and combustion, the unstructured grid with better adaptability was used, and a local mesh encryption method is presented to more accurately simulate the combustion characteristics when the flow distribution changes drastically, such as the burner area. In the simulation process, the approximate grid-independent solution is obtained by gradually thinning the grid, and the specific grid model is shown in fig. 2.

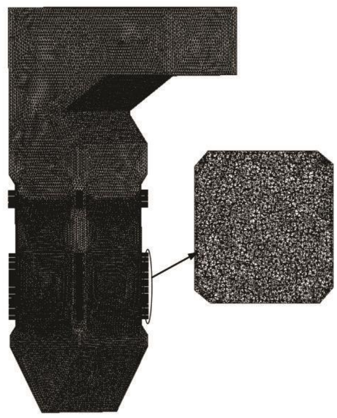

Figure 2. Mesh model

Mathematical model

In the numerical simulation of pulverized coal combustion in the furnace, the standard k-ε equation of both processes was selected to simulate the gas phase turbulence [27]. The near-wall area of low Reynolds number was processed by Standard Wall Function. The Lagrangian discrete model was used to simulate the effect of the gas-solid two-phase of coal powder and air, and the Two-interrelated-rates were analyzed in the pulverized coal volatilization. The mixture-reaction was selected to simulate the combustion of gas phase. The kinetics/diffusion control reaction rate model was selected for coke combustion. The P-1 model was selected for the radiation in the furnace [28]. The diameter hypothesis of pulverized coal particles follows the distribution of rosin-rammler.

The mixed fractional-probability density function method [29] simplifies combustion to a hybrid problem. The instantaneous thermochemical state of the fluid is associated with a conserved quantity and a mixed fraction, $\overline{f}$. The transport equation of mixed fractions is:

The equation of the average mixed score (time average) $\overline{f}$ are:

$$\frac{\partial}{\partial t}\left(\rho \overline{f}\right)+\nabla\left(\rho \overline{v}\overline{f}\right)=\nabla\left(\frac{\mu_t}{\sigma_t}\nabla \overline{f}\right)+S_m+S_{\text{user}} \tag{1}$$

$$\frac{\partial}{\partial t}\left(\rho \overline{f'^2}\right)+\nabla\left(\rho \overline{v}\,\overline{f'^2}\right)=\nabla\left(\frac{\mu_t}{\sigma_t}\nabla \overline{f'^2}\right)+C_g\mu_t\left(\nabla^2 \overline{f}\right)-C_d\rho\frac{\varepsilon}{k}\overline{f'^2}+S_{\text{user}} \tag{2}$$

where $f' = f - \overline{f}$, S_{user} is the source term. $\sigma_t = 0.85$, $C_g = 2.86$, $C_d = 2.0$.

A two-step competitive reaction model was used in the analysis of pulverized coal volatilization. The rate of volatilization is:

$$v_{\text{vol}} = (k_1 R_1 + k_2 R_2) m_c \tag{3}$$

where m_c is the quality of raw coal in pulverized coal particles. For the reaction equivalent ratio, the coefficients k_1 and k_2 are 0.3 and 1.0, respectively.

The kinetics/diffusion control reaction rate model was selected for coke combustion. The combustion rate of coke particles in this model is not only affected by the rate of the chemical reaction but also affected by the diffusion rate. The diffusion rate, D_0, expression is:

$$D_0 = C_1 \frac{\left[\left(T_p + T_\infty\right)/2\right]^{0.75}}{d_p} \tag{4}$$

The expression of the chemical (kinetic) reaction rate, R, is:

$$R = C_2 \mathrm{e}^{-(E/\mathrm{R}T_p)} \tag{5}$$

The combustion rate of coke particles is:

$$\frac{\mathrm{d}m_p}{\mathrm{d}t} = -\pi d_p^2 p_{ox} \frac{D_0 R}{D_0 + R} \tag{6}$$

where p_{ox} is the partial pressure of the oxidant and R is the rate constant.

Modeling NO_x formation and reduction

The NO_x in the furnace mainly refers to NO, NO_2, and N_2O, in which NO accounts for about 90%. According to the generation mechanism, NO_x can be divided into subthermal type NO_x, rapid NO_x, and fuel type NO_x. The amount of rapid NO_x generation is very small, only 5% of the total NO_x generation. In the study, the thermal NO_x and fuel type NO_x are mainly considered. Thermal NO_x is generated by the reaction of N_2 and O in the air at high temperatures (N_2 + O → N + NO, O_2 + N → NO + O). The rate of formation is related to the temperature, that is, temperature has a significant effect on NO_x generation. When the temperature is more than 1800 K, the amount of NO_x generated increases sharply with the temperature rises. In the actual operation of the pulverized coal combustion furnace, the uneven temperature in the furnace leads to high temperatures in some sectors, resulting in a large number of fuel NO_x generation, and good combustion organization can effectively reduce the thermal NO_x. The fuel type NO_x is derived from two parts of the volatile homogeneous combustion and coke heterogeneous combustion, accounting for about 75% of the total NO_x generation. Volatile nitrogen is released shortly after the volatiles are released and then produce compounds such as HCN and NHi. On the one hand, HCN and NHi are oxidized to form NO_x in oxidizing atmosphere, and on the other hand, these nitrogen compounds can undergo a complex reaction and reduce NO_x to N_2 in reducing atmosphere. Coke nitrogen release after the volatile nitrogen, the formation of coke NO_x depends on the competition results of coke nitrogen oxidation process and the reduction of the generated NO_x by the coke surface. During the pyrolysis of coke, it reacts with oxygen in the thin layer of the surface of the coke particles and partially generates NO_x. At the same time, the NO molecules in the flue gas are adsorbed on the surface of the coke ($NO + \alpha(–C) \rightarrow 0.5N_2 + (2\alpha – 1)CO + (1 – \alpha)CO$). Thus, the effect of coke nitrogen on NO_x release depends on the specific situation. In this study, the post-treatment method for NO_x generation simulation is used to simulate the release of NO_x.

Result analysis

Typical characteristics of combustion in the furnace

Figure 3 shows the temperature distribution of the width of the furnace in the central longitudinal section and the different positions of the horizontal cross-section in the original conditions. The unit of temperature is K. It can be seen that the pulverized coal is sprayed into the hearth from the primary air outlet and is strongly mixed with the secondary air, and heated by the high temperature flue gas. After entering the furnace for 1~2 m, the volatiles start to decompose, burn and release heat. the surrounding flue gas is heated by convection and radiant heating, so the 1800 K local high temperature area is formed in the vicinity of the nozzle, and the four jet interacts with each other, the adjacent pulverized coal flow ignited each other, forming a spiral rotation of the rising airflow in the center of the furnace and the inverted V-type temperature distribution characteristic is formed on the cut surface. In addition, the stove combustion of the furnace controls the temperature of the burner area and coal further burns in the elevation of about 28 m height of the exhausted wind area, high temperature area extends to the elevation of 40 m, and the high temperature area is moved to the center of the furnace. The horizontal cross-section temperature's uniformity is good for the safe and efficient operation of boiler.

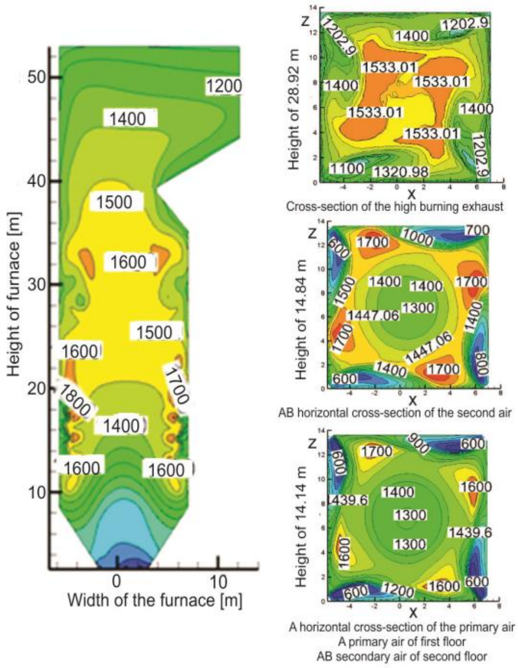

Figure 3. The temperature distribution of a furnace center cross section and different height

Effect of pulverized coal concentration on NO_x emission

The concentration of pulverized coal affects the precipitation of volatiles, the rate of the combustion reaction, the heat transfer between the particles and the gas phase, which further influences the precipitation of HCN and its transformation direction [4]. In this paper, the concentration of pulverized coal is increased or decreased respectively on the basis of the original working condition, in which the concentration of pulverized coal is 0.467 kg/kg, and the NO_x release characteristics with different pulverized coal concentrations were compared.

Figure 4 shows the formation of CO in the furnace at three different pulverized coal concentrations. As shown in fig. 4, the high concentration area of CO exists in the primary inlet area (elevation 10~15 m) because of the incomplete combustion of a large number of pulverized coal, with the secondary air injection and combustion, CO content reduces along the height of the furnace. The second peak of CO content appears at 22 m and then decreases again with the reaction in the furnace. With the increase of pulverized coal concentration, the incomplete combustion of pulverized coal is more serious. The peak value of CO content increases from 0.0352% to 0.0587% as the concentration of pulverized coal increases from 0.421 kg/kg to 0.532 kg/kg. The concentration of CO can create a reducing atmosphere which could inhibit the formation of NO_x.

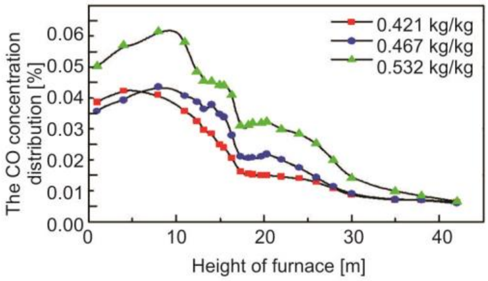

Figure 4. The CO concentration distribution under different pulverized coal concentration

After the pulverized coal is injected into the furnace, a large amount of volatiles are volatilized at about 2 m from the inlet and the heat is released, and the nitrogen compounds such as HCN are released. Figure 5 shows the mass fraction of HCN in different working conditions. The concentration of HCN reached the highest at 2~4 m, and the HCN concentration in the burner area increases with the increase of pulverized coal concentration. As the oxidation or reduction of HCN proceeds, the concentration decreases gradually along with the height of the furnace. As the increase of CO and other reducing gases could increase the conversion rate of HCN, which can effectively reduce the release of NO_x, the concentration of HCN in the upper part of the furnace decreases with the increase of pulverized coal concentration.

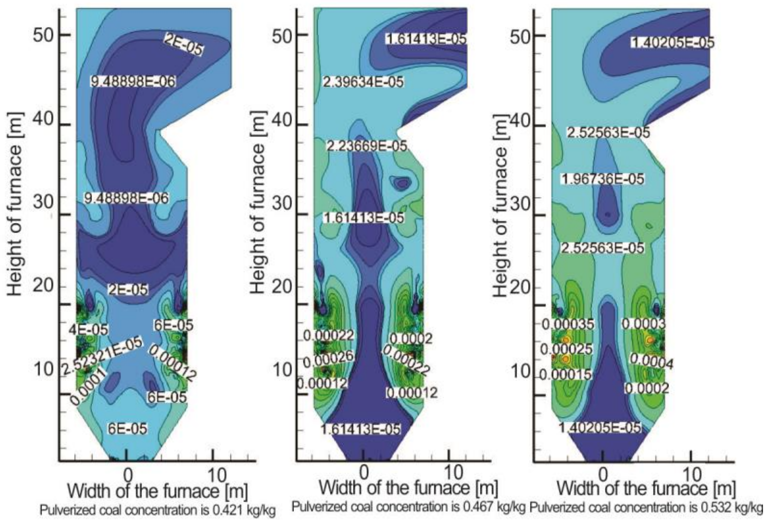

Figue 5. The HCN mass fraction under different pulverized coal concentration

Figure 6 shows the mass concentration distribution of NO_x in the furnace at different pulverized coal concentrations. It can be seen that the NO_x concentration in the furnace is highest at 2~4 m from the inlet, and gradually decreases along with the height of the furnace. In the burner zone, the large amount of volatile nitrogen releases, causing a sharp increase of NO_x concentration. As the reducing gas and the coke particle concentration increase in the furnace, the NO_x is reduced in large quantities.

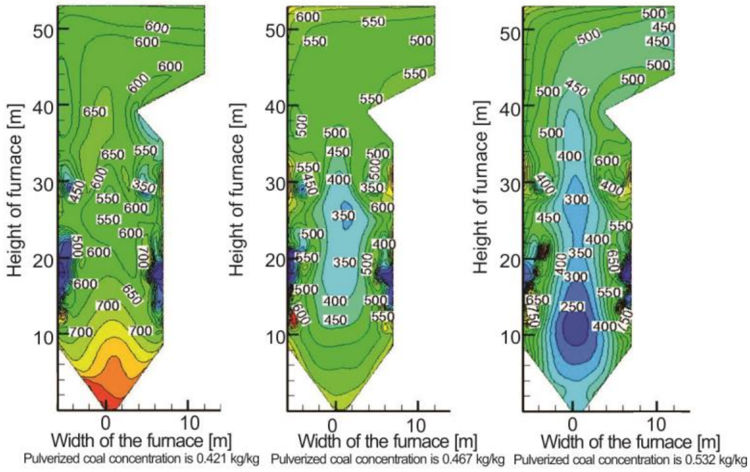

Figure 6. The NO_x concentration under different pulverized coal

With the increase of pulverized coal concentration, the concentration of NO_x in the furnace is greatly reduced. On the one hand, the increase of CO production, the intermediate product HCN is converted to N_2 along the HCN → NCO → N → N_2 route in the strong reducing atmosphere, and the CO reacts with the generated NO: $CO + NO \rightarrow CO_2 + 1/2N_2$, that is, high CO concentration can reduce the amount of NO_x generated. On the other hand, the overall concentration of HCN in the furnace is relatively low at high coal concentration conditions according to fig. 5. Finally, as the concentration of pulverized coal increases, the concentration of coke particles increases, and some of the transformed NO is adsorbed and reduced. Therefore, the conversion of NO_x is low.

Table 3 shows the temperature and NO_x concentration of the furnace under different pulverized coal concentrations. As the concentration of pulverized coal increases from 0.421 kg/kg to 0.532 kg/kg, the temperature variation of the furnace is not obvious. However, the mass concentration of NO_x in the furnace outlet decreases from 644.97 mg/m^3 to 366.07 mg/m^3, which decreases by 43.30%. It can be seen that the proper increase of the pulverized coal concentration can effectively reduce the release of NO_x under the premise of ensuring the safe operation of the boiler.

Effect of separated overfire air velocities on NO_x release

The exhausted wind has an important effect on the formation of NO_x in the combustion of pulverized coal in the furnace. The air emission characteristics of combustion air at 33 m/s, 38 m/s, 43 m/s, and 48 m/s were investigated under the same conditions.

Figure 7 shows the temperature of the furnace under different separated over fire air velocities. The temperature trend of the furnace center is the same when the separated over

Table 3. The temperature and NO_x concentrations under different pulverized coal concentrations

Pulverized coal concentration [kgkg^{-1}]	Maximum temperature in the furnace [K]	Outlet temperature [K]	Maximum NO_x concentration in the furnace [mgm^{-3}]	Outlet NO_x concentration [mgm^{-3}]
0.421	1930	1124.49	1765.72	644.97
0.467	1962	1103.28	1673.42	520.22
0.532	1970	1087.49	1771.73	366.07

fire air is different. The peak value appears at 18~22 m. With the increase of the air velocity, the second temperature peak appears at 30 m, and the peak temperature of the furnace center decreases as the separated over fire air velocity increases, which can reduce the formation of thermal NO_x.

The CO mass fraction in different working conditions is shown in fig. 8. When the separated over fire air velocity is increased and the secondary air is reduced correspondingly. The CO concentration at different separated over fire air velocities has the same trend. The concentration of CO is obviously increased at 10~20 m, where the oxygen content is low and the fuel is rich.

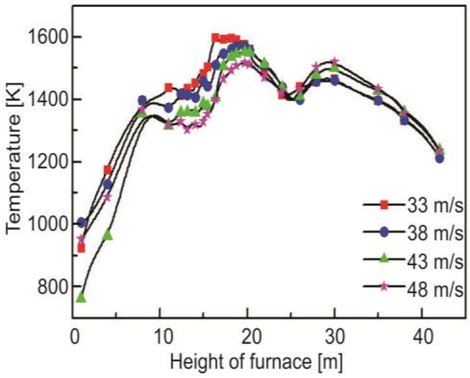

Figure 7. The temperature distribution under different separated over fire air velocity

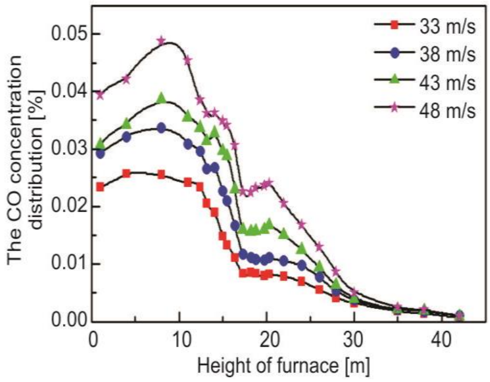

Figure 8. The CO distribution under different separated over fire air velocities

Figure 9 shows the generation of NO_x under different operating conditions and the release of NO_x at the furnace outlet. It was found that the trend of NO_x concentration along the height direction was the same, which decreased firstly and then reached the lowest value at 18 m due to the reduction of CO, and the NO_x concentration in the furnace area of 18 m or more increases due to the high temperature in the region. The concentration of NO_x decreases significantly as the separated over fire air velocity increases. On the one hand, the hypoxic atmosphere caused by the reduction of the secondary air inhibits HCN from being oxidized to generate NO_x, on the other hand, high concentration of CO and coke particles formed by the reduction of HCN and the generated NO is reduced to N_2, which can reduce the fuel type NO_x generation to a large extent. The NO_x concentration on the outlet section of the furnace decreases from 624.67 mg/m^3 to 476.87 mg/m^3 as the separated over fire air velocity is increased from 33 m/s to 48 m/s, that is, separated over fire air velocity can effectively reduce the release of NO_x.

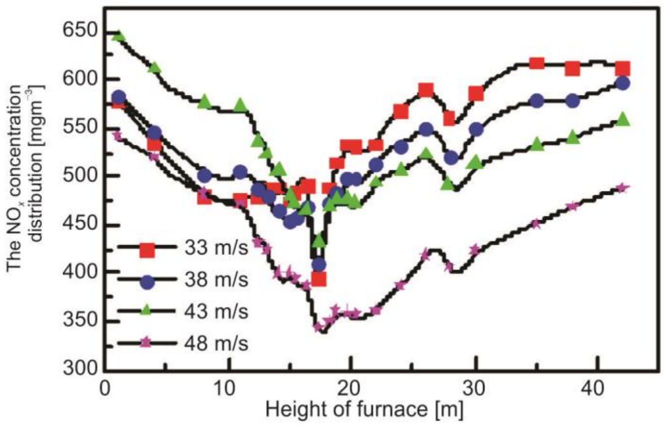

Figure 9. The NO_x distribution under different separated over fire air velocity

Effect of boiler load on NO_x release

The release characteristics of NO_x in the furnace were compared under 50%, 80%, and 100% load, respectively, without changing the amount of air volume and changing the secondary air volume proportionally.

The coal-feed and air distribution will correspondingly change as the boiler load changes. Figure 10 shows the temperature distribution inside the furnace under different boiler loads. It can be seen from fig. 10 that there is no obvious temperature variation at the height of 18~27 m of the furnace center under different boiler loads. However, the bottom temperature of 50% load is higher than 80% load, which is easy to cause the bottom slag of the cold ash bucket.

Figure 11 shows the concentration of CO under different boiler loads. As shown in fig. 11, the trend of the CO concentration along the furnace height direction is nearly the same under different boiler loads, which increases firstly and then decreases, and finally tends to be stable. The concentration of CO is the lowest under 100% load in the lower area of the furnace. As the boiler load decreases, the secondary air decreases in proportion, and the further combustion of pulverized coal is not sufficient. Therefore, much CO is generated in the lower part of the furnace under lower boiler load condition.

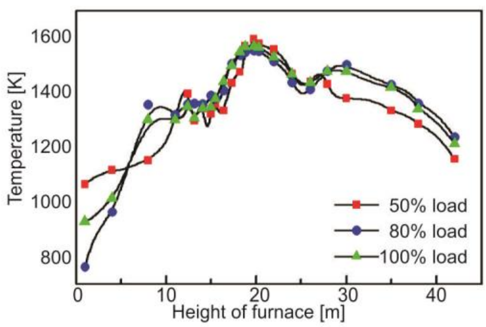

Figure 10. The temperature distribution of the furnace center section under different load

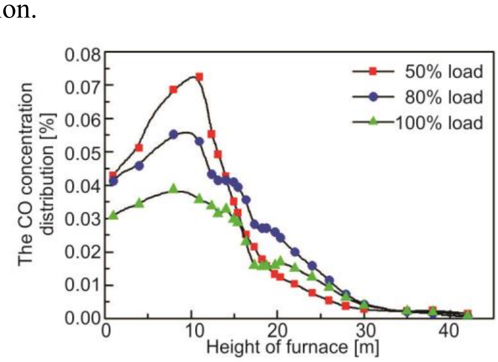

Figure 11. The CO concentration distribution under different load

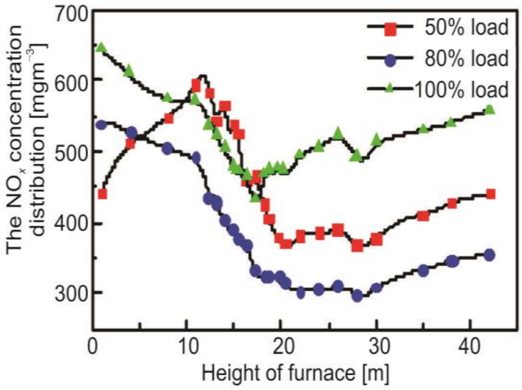

Figure 12. The NO_x concentration distribution under different load

Figure 12 shows the generation of NO_x under different boiler loads. As shown in fig. 12, the NO_x concentration in the furnace decreases firstly and then increases, and the mass concentration of NO_x is the lowest under 80% load. Compared with the temperature distribution in fig. 9, the overall temperature in the lower part of the furnace is lowest under 80% boiler load, and the concentration of CO is relatively high, so little NO_x is generated.

Table 4 shows the change in temperature level and NO_x concentration under different boiler loads. As the boiler load decreases, the temperature of the furnace gradually decreases. The mass concentration of NO_x on the outlet of furnace decreases from 520.22 mg/m^3 to 315.38 mg/m^3 as the boiler load decreases from 100% to 80%.

Table 4. The temperature of the furnace and NO_x concentrations under different load

Boiler load [%]	Maximum temperature in the furnace [K]	Outlet temperature [K]	Maximum NO_x concentration in the furnace [mgm^{-3}]	Outlet NO_x concentration [mgm^{-3}]
50	2068	1058.86	1969.74	379.73
80	2092	1087.49	1591.75	315.38
100	1930	1103.28	1673.42	520.22

Simulation verification

To verify the reliability of simulation results, the flue gas temperature and NO_x concentration at the boiler exit was measured. Figure 13 compares the simulated results with the experimental data. It can be seen from fig. 13 that the flue gas temperature simulated at the exit of the furnace is consistent with the trend of the measured temperature. The simulated temperature is about 20 K less than the measured temperature, which is within the reasonable error range. The NO_x concentration at the furnace exit measured is consistent with that of the simulated NO_x concentration. When the boiler load is 80%, the temperature in the furnace is reasonable and the NO_x emission at the furnace outlet is low, so the combustion in the furnace is relatively good. Figure 13 proves that the numerical simulation results are basically in line with the actual measured results, and the calculation results are reliable.

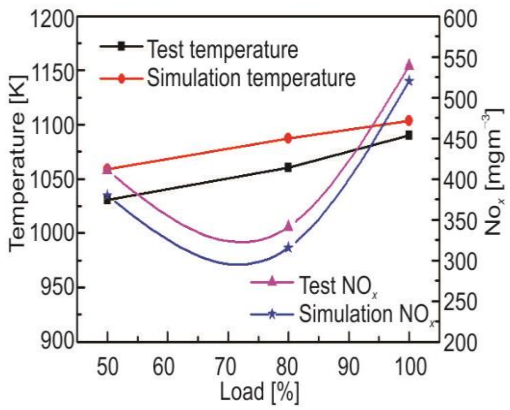

Figure 13. Comparison of calculation results and experimental data

Conclusions

In this paper, the influence of coal concentration, staged air distribution and boiler loads on nitrogen oxides generation were analyzed, and the simulated results were compared with the measured one, the following conclusions can be obtained.

- A large number of volatiles are burned out after the pulverized coal is crushed into the boiler about 1~2 m. The center of the furnace spirally rises to form the inverted V-type temperature distribution, and the local high temperature can be up to 1930 K at 100% boiler load.
- Increasing the pulverized coal concentration can effectively inhibit the release of NO_x. the average NO_x concentration on the furnace outlet decreases from 644.97 mg/m^3 to 366.07 mg/m^3 as the concentration of pulverized coal increases from 0.421 kg/kg to 0.532 kg/kg.
- The separated over fire air velocity on the tangential boiler combustion process has an important effect on the release of NO_x. An appropriate increase in separated over fire air velocity could reduce NO_x emissions on the furnace outlet.

Nomenclature

A	– ash content, [%]
C	– concentration, [molcm^{-3}]
d	– particle diameter, [mm]
D	– diffusion coefficient, [m^{2}s^{-1}]
f	– mixed score
k	– kinetic energy of turbulence, [m^{2}s^{-2}]
M	– moisture, [%]
R	– general gas constant, [Jmol^{-1}K^{-1}]
S	– source term
T	– fluid temperature, [K]
t	– time, [s]
V	– volatile matter production, [%]
v	– mean velocity, [ms^{-1}]

Greek symbols

ε	– dissipation of turbulent kinetic enegy, [m$_2$s^{-3}]
ρ	– density, [kgm^{-3}]
μ	– dynamic viscosity, [Pa s]

Subscripts

ad	– air dry basis
ar	– as received basis
daf	– dry ash free basis
g	– gas phase
user	– user-defined
vol	– volatile matter
ox	– oxidant

References

[1] Korytnyi, E., *et al*., Computational Fluid Dynamic Simulations of Coal-Fired Utility Boilers: An Engineering Tool, *Fuel, 88* (2009), 1, pp. 9-18
[2] Agraniotis, M., *et al*., Numerical Investigation on the Combustion Behaviour of Pre-Dried Greek Lignite, *Fuel, 88* (2009), 12, pp. 2385-2391
[3] Shen, Y. S., *et al*., A Three-Dimensional Numerical Study of the Combustion of Coal Blends in Blast Furnace, *Fuel, 88* (2009), 2, pp. 255-263
[4] Song, Y. H., *et al*., Nitric Oxide Formation during Pulverized Coal Combustion, *Combustion Science and Technology, 28* (1982), 1, pp. 37-39
[5] Agraniotis, M., *et al*., Experimental Investigation on the Combustion Behaviour of Pre-Dried Greek Lignite, *Fuel, 90* (2009), 9, pp. 1071-1079
[6] Sheng, C., *et al*., A Computational Fluid Dynamics Based Study of the Combustion Characteristics of Coal Blends in Pulverised Coal-Fired Furnace, *Fuel, 83* (2004), 11, pp. 1543-1552
[7] Yin, C., *et al*., Investigation of the Flow, Combustion, Heat-Transfer and Emissions from a 609 MW Utility Tangentially Fired Pulverized-Coal Boiler, *Fuel, 81* (2002), 8, pp. 997-1006
[8] Achim, D., *et al*., Numerical Investigation of Full Scale Coal Combustion Model of Tangentially Fired Boiler with the Effect of Mill Ducting, *Heat And Mass Transfer, 46* (2009), 1, pp. 1-13
[9] Xiang, J., *et al*., An Experimental Research on Performance of Nitrogen Oxide Emission from Boiler, *Proceedings of the CSEE, 20* (2000), 9, pp. 80-84

[10] Yang, W. J., *et al*., Tertiary Air Operation Optimization Aiming at Low NOx Combustion in Boiler, *Journal of Zhejiang University :Engineering Science, 42* (2008), 7, pp. 1227-1230
[11] Zhou, H., *et al*., Numerical Simulation of the NOx Emissions in a 1000 MW Tangentially Fired Pulverized-Coal Boiler: Influence of the Multi-group Arrangement of the Separated over fire air, *Energy & Fuels, 25* (2011), 5, pp. 2004-2012
[12] Park, H. Y., *et al*., Coupled Fluid Dynamics and Whole Plant Simulation of Coal Combustion in a Tangentially-Fired Boiler, *Fuel, 89* (2010), 8, pp. 2001-2010
[13] Wei, L H., *et al*., An Experimental Investigation on Nitrogen Emission Properties of Micro-Pulverized During Pyrolysis, *Proceedings of the CSEE 26*, (2006), 7, pp. 62-66
[14] Wang, Y. Z., *et al*., Experimental Study on the Characteristics of the Nitrogen Releasing from the Pulverized Coal Combusting in the One-Dimensional Boiler, *Journal of China Coal Society, 29* (2004), 6, pp. 726-730
[15] Wang, X. D., *et al*., Experimental of Effects of Boiler Structures and Burner Models On Nox Emission From Coal-Fired Boiler, *Journal of China Coal Society, 32* (2007), 9, pp. 984-988
[16] Jarquin-Lopez, G., *et al*., Analytical and Experimental Research for Decreasing Nitrogen Oxides Emissions, *Applied Thermal Engineering, 29* (2009), 8-9, pp. 1614-1621
[17] Xiao, H. P., *et al*., Effect of Combustion Adjustment on NOx Emission and Boiler Efficiency, *Proceedings of the CSEE, 31* (2011), 8, pp. 1-31
[18] Zhou, J. H., *et al*., Application of Air-staged and Low NOx Emission Combustion Technology in Plant Boiler, *Proceedings of the CSEE, 23* (2010), 5, pp. 19-23
[19] Li, Z. Q., *et al*., Influence of Declivitous Secondary Air on Combustion Characteristics of a Down-Fired 300 MW Utility Boiler, *Fuel, 89* (2010), 2, pp. 410-416
[20] Zeng, L. Y., *et al*., Numerical Simulation of Combustion on Characteristics and NOx Emission in a 300 MW Utility Boiler with Different Outer Second-Air Bane Angles, *Energy & Fuels, 24* (2010), 10, pp. 5349-5358
[21] Fang, Q. Y., *et al*., Numerical Simulations on the Slagging Characteristics in a Down-Fired, Pulverized Coal Boiler Furnace, *Fuel Processing Technology, 91* (2010), 1, pp. 88-96
[22] Belosevic, S., *et al*., Three-Dimensional Modeling of Utility Boiler Pulverized Coal Tangentially Fired Furnace, *International Journal of Heat and Mass Transfer, 49* (2006), 19-20, pp. 3371-3378
[23] Choi, C. R., Chang, N. K., Numerical Investigation on the Flow, Combustion, and NOx Emission Characteristics in a 500 MW Tangentially Fired Pulverized-Coal Boiler, *Fuel, 88* (2009), 9, pp. 1720-1731
[24] Chen, T. J., *et al*., Numerical Simulation on the Optimization of Closing-to-Wall Air in a 660 MW Front and Rear Wall Opposed Coal-Fired Boiler, *Proceedings of the CSEE, 35* (2015), 20, pp. 5265-5271
[25] Wang, W. S., *et al*., Numerical Simulation on the NOx Release Characteristics During the Combustion of Power-Quality Anthracite in Supercritical Boiler, *Journal of China Coal Society, 37* (2012), 2, pp. 310-315
[26] Liu, Y. M., *et al*., Numerical Study on NOx Emission Characteristics of a 600 MW Opposed Firing Boiler, *Journal of Chinese Society of Power Engineering, 35* (2015), 5, pp. 341-347
[27] Tao, W. Q., *Numerical Heat Transfer*, Xi'an Jiaotong University Press, Xi'an, China, 2003
[28] Wang, F. J., *Computational Fluid Dynamics Analysis, The principle and application of CFD Software*, Tsinghua University Press, Beijing, China, 2004
[29] Dong, C., *et al*., Numerical Modeling of the Gasification Based Biomass Co-Firing in a 600 MW Pulverized Coal Boiler, *Applied Energy, 87* (2010), 9, pp. 2834-2838

Paper submitted: October 10, 2019
Paper revised: November 22, 2019
Paper accepted: December 9, 2019